

Plasmon-induced ZnO-Ag/AgCl photocatalyst for degradation of tetracycline hydrochloride

Nan Cui^a, Amir Zada^b, Jiahe Song^a, Yuzhuo Yang^a, Minghui Liu^a, Yan Wang^a, Yuxin Wu^c, Kezhen Qi^{a,d,*}, Rengaraj Selvaraj^{e,*}, Shu-yuan Liu^c, Ge Jin^{c,*}

^aInstitute of Catalysis for Energy and Environment, College of Chemistry and Chemical Engineering, Shenyang Normal University, Shenyang, China, Tel. 86-24-86578847; emails: qkzh2003@aliyun.com (K. Qi), 15842743380@163.com (N. Cui), songjiahe1998@163.com (J. Song), 1599986563@qq.com (Y. Yang), lmh15241637597@163.com (M. Liu), wangyan11287@mail.nankai.edu.cn (Y. Wang)

^bDepartment of Chemistry, Abdul Wali Khan University Mardan, Mardan, Pakistan, email: amirzada@awkum.edu.pk (A. Zada)

^cDepartment of Pharmacology, Shenyang Medical College, Shenyang 110034, China, emails: jing1026@163.com (G. Jin), 1339107096@qq.com (Y. Wu), liushuyuan@symc.edu.cn (S.-y. Liu)

^dKey Laboratory of Advanced Energy Materials Chemistry (Ministry of Education), College of Chemistry, Nankai University, Tianjin 300071, China

^eDepartment of Chemistry, College of Science, Sultan Qaboos University, P.O. Box: 36 Al-Khoudh, Muscat, P.C. 123 Sultanate of Oman, Tel. 00968-2414-2436; email: srengaraj1971@yahoo.com (R. Selvaraj)

Received 15 July 2021; Accepted 6 November 2021

ABSTRACT

The release of a large number of antibiotics to the environment has created a shade of sorrow in the scientific community. This work reports the preparation of efficient plasmon-induced ZnO-Ag/AgCl photocatalysts by in-situ coprecipitation and hydrothermal methods, and applied for the degradation of tetracycline hydrochloride antibiotic under visible light irradiation. The ZnO-Ag/AgCl composites were characterized by XRD, TEM-EDS, DRS, XPS and PL. The photocatalytic efficiency of ZnO was significantly improved by introducing proper amount of Ag/AgCl. The improved photocatalytic activity is due to the surface plasmon resonance effect of Ag metal and charge separation in the nanocomposite material. The obtained results showed that ZnO-Ag/AgCl photocatalyst had higher photocatalytic activity compare to pure ZnO. The amount optimized sample containing 30% Ag/AgCl decomposed 80.7% tetracycline hydrochloride in 2 h. From trapping experiments, it was concluded that super oxide anions were the main degrading species involved in the degradation of tetracycline hydrochloride. Finally, charge transfer mechanism was proposed based on the obtained results and active species involved in the degradation process. In conclusion, the synthesized ZnO-Ag/AgCl composite photocatalyst has a good potential for environmental remediation.

Keywords: ZnO-Ag/AgCl; Tetracycline hydrochloride; Photocatalytic activity; Visible light

1. Introduction

The rapid development of industry and economy has caused severe water pollution crisis. The introduction of

different antibiotics as emerging pollutants to the external environment has threaten human life and disturbed the normal ecosystem in the recent years. Especially, the

* Corresponding authors.

tetracycline hydrochloride (TC-HCl) found in the effluents of hospitals and livestock breeding centres has caused large-scale water pollution and posed serious threats to aquatic animals and plants [1]. Conventional treatment methods such as adsorption, microbial removal and electrochemical techniques have been exercised extensively but no one gained enough popularity due to the incomplete removal, costly materials, high energy requirements and time consuming characteristics [2]. Therefore, more advanced, efficient and green techniques are instantly required to eradicate these emerging pollutants for the protection of water ecosystem and aquatic life.

Photocatalysis has been matured in the degradation of organic pollutants owing to its high efficiency and eco-friendly characteristics. The availability of plenty solar energy is a cost effective factor to commercialize photocatalysis for energy consumption and environmental remediation [3]. Different photocatalysts have been applied for pollutants degradation with some remarkable deliveries, such as TiO_2 , ZnO, $\text{g-C}_3\text{N}_4$, CdS etc. [4–19]. Among these photocatalysts, ZnO has attracted massive attention due to its non-toxic nature, low cost, excellent physical stability, high hydrophobicity, oxidant power, favorable band edge positions, and environmental sustainability [20–22]. Unfortunately, its high band gap of 3.21 eV and high recombination rate of photogenerated carriers do not allow it to harvest major portion of the electromagnetic radiations for high efficiency photocatalysis. Therefore, the modification of ZnO has become a hot topic in the scientific research.

The introduction of metal and non-metal dopants, construction of proper heterojunction with other semiconductors and loading of noble metals on the surface of ZnO have been exercised by many researchers for improved photocatalytic performance [23–31]. Especially, the introduction of silver/silver halide (Ag/AgX, X = Cl, Br, I) have delivered excellent photocatalytic degradation activity under visible light irradiation as the pore channels between Ag and AgCl have surface plasma resonance effect to reduce recombination of the electron-hole pairs. Modification with Ag also bends the band of the semiconductor at the interface of the metal and semiconductor to form Schottky barriers, which can accelerate the electron transfer between the interface of the components of composite [32–34]. Further, the introduction of Ag metal has many advantages such as low cost, superior electrical and thermal conductivities.

By exploiting the effective coordination of Ag^+ with ZnO to enhance its chemical stability, we loaded Ag/AgCl as a nanocomposite material on the surface of ZnO by in-situ coprecipitation and hydrothermal methods. The as prepared ZnO-Ag/AgCl composite was applied for the photocatalytic degradation of tetracycline hydrochloride. The determination of the active species involved in the degradation of tetracycline hydrochloride was employed to understand the charge transfer mechanism in ZnO-Ag/AgCl under visible light irradiation. The enhanced photocatalytic activities of ZnO-Ag/AgCl are attributed to the synergetic effect of Ag and AgCl to harvest visible light photons and effectively reduce exciton recombination and has potential environmental applications.

2. Experimental part

2.1. Synthesis

In a typical synthesis, 1.317 g $\text{Zn}(\text{CH}_3\text{COO})_2$ and 0.59 g NaOH were dissolved in 20 mL ultrapure water. The mixture was put in 50 mL autoclave and heated at 140°C for 12 h in an oven to obtain ZnO. After the preparation of ZnO, ZnO-Ag/AgCl nanocomposite was prepared by in-situ coprecipitation method. 0.2 g ZnO were dispersed in 60 mL ultrapure water for 20 min under sonication and then different volumes of silver nitrate (0.1 M, 1–7 mL) solution were dropwise introduced to the above suspension under stirring for 30 min at room temperature. After that, different amounts of KCl were added and the mixed solution was placed under xenon light source for 1 h. Finally, the mixture was centrifuged at the speed of 8,000 r/min and the precipitate was dried in a vacuum oven at 60°C overnight to get gray black samples. According to the volume of silver nitrate and KCl added, the theoretical weight percent amount of Ag/AgCl loading was calculated to be 5, 10, 15, 20, 25, 30 and 35.

2.2. Characterization

Japanese physical smart Lab (3) intelligent X-ray diffractometer ($\text{Cu } k\alpha$, $\lambda = 1.54056 \text{ \AA}$) was used to characterize the catalyst samples. X-ray photoelectron spectroscopy (XPS) was measured on PHI1600 XPS (US) instrument and the obtained binding energies were calibrated with binding energy of adventitious carbon. High resolution transmission electron microscopy (HRTEM) was carried out with JEOL-JEM-2100F electron microscope. The UV-Vis absorption spectra were collected on the Shimadzu UV3100 (Japan) spectrophotometer using BaSO_4 as reference material. The photoluminescence (PL) spectra of ZnO and ZnO-Ag/AgCl samples were studied on a Varian-Cary solar eclipse spectrometer with an excitation wavelength of 325 nm.

2.3. Photocatalytic activity measurements

TC-HCl was selected as a model pollutant. A series of photocatalytic degradation experiments were conducted to evaluate the performance of the photocatalysts under visible light ($\lambda > 400 \text{ nm}$). 32 mg of the photocatalysts were dispersed in 50 mL TC-HCl (20 mg/L) solution and stirred in dark for 30 min to allow adsorption of pollutants on the surface of the photocatalysts. During irradiation, 5 mL of the sample solution were drawn after every 20 min and centrifuged three times at 9,000 rpm for the measurement of the pollutant concentration with visible spectrophotometer. The same experiment was repeated with different dosage of photocatalysts under different pH values in the presence of different anions. The removal efficiency of TC-HCl was calculated by the following formula:

$$\eta\% = \frac{C_0 - C_t}{C_0} \times 100 \quad (1)$$

where η is the degradation efficiency of TC-HCl, C_t is the concentration after t -degradation time, and C_0 is the initial concentration of TC-HCl.

3. Results and discussion

3.1. XRD analysis

Fig. 1 shows the XRD patterns of ZnO-Ag/AgCl samples prepared with different contents of Ag/AgCl. The peaks of all samples correspond to the (100), (002), (101), (102), (110), (103) and (112) crystal planes of ZnO are located at 31.78°, 34.42°, 36.26°, 47.54°, 56.58°, 62.84° and 67.97°, respectively, according to the standard PDF card (36–1451) [35]. The XRD peaks at 38.16°, 44.31°, 64.45° and 77.51°, are respectively corresponded to (111), (200), (220) and (311) crystal planes of Ag according to the standard PDF card (04–0783). There is no characteristic peak of AgCl in the 5%–20% range due to its large dispersion on the surface of ZnO. However, with increase in the amount up to 25%, the diffraction peak of AgCl begins to appear in the 25%-ZnO-Ag/AgCl sample, and the intensity of the corresponding peak of ZnO and Ag gradually decreases. No characteristic peaks of other substances were observed in the prepared samples, indicating that the samples are of high purity and Ag/AgCl is loaded on ZnO substrate successfully.

3.2. Transmission electron microscopy

The TEM image of ZnO-Ag/AgCl-30% is shown in Fig. 2. It is clear that the prepared catalyst is the form of nanosheets with different sizes (Fig. 2a). At high magnification, the Ag/AgCl particles with a diameter of 3–5 nm can be observed on the surface of ZnO (Fig. 2b). The corresponding energy spectrum of the sample is shown in Fig. 2c. The characteristic peaks of Zn, O, Cl and Ag elements appear in the spectrum, which indicates the successful preparation of Ag/AgCl loaded ZnO photocatalysts. It can be seen from Fig. 2c that the peak intensity of Ag element is almost higher than that of Zn element, which is caused by the attachment of Ag/AgCl on the surface of ZnO, and the test value of Ag in EDS detection becomes larger.

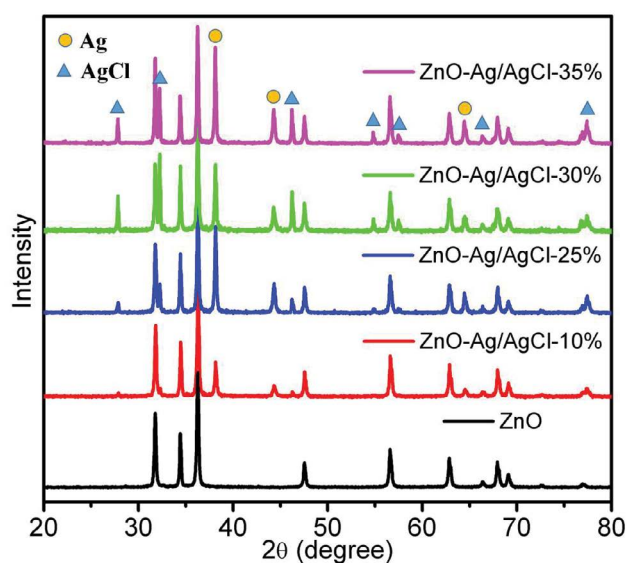


Fig. 1. XRD patterns of ZnO and ZnO-Ag/AgCl/Ag samples.

3.3. UV-Vis DRS

Diffuse reflectance spectra were measured to explore the light absorption capacity of the samples and the results are shown in Fig. 3. The absorption edge of pure ZnO is at 400 nm with obviously no absorption in the visible region, and the maximum absorption peak in the given region is slightly higher than that of the nanocomposite samples. The gray ZnO-AgCl sample shows higher light absorbance than that of pure ZnO. All samples of ZnO-Ag/AgCl show absorption in the visible region at 420 nm due to the surface plasmon resonance effect of Ag and the intensity of absorption increases with increase in the amount of Ag/AgCl. Thus the introduction of Ag/AgCl obviously increases the ability of ZnO to harvest visible light for enhanced photocatalytic activity.

3.4. X-ray photon spectroscopy

The XPS data were taken to evaluate the elemental composition and oxidation states of the sample (Fig. 4). Fig. 4a shows the survey spectra of Zn 2p, O 1s, Ag 3d and Cl 2p of the ZnO-Ag/AgCl-30%. In Fig. 4b, the XPS spectrum of Zn 2p is deconvoluted into two characteristic peaks at 1,021.4 and 1,044.6 eV corresponded to Zn 2p_{3/2} and Zn 2p_{1/2}} respectively. This indicates that the valence state of Zn is +2 in the complex [36]. Fig. 4c shows that the high-resolution O 1s XPS spectrum can be simulated into two peaks with binding energies 530.3 and 531.9 eV and are corresponded to the oxygen of Zn-O [37]. The two characteristic peaks at 367.5 and 373.5 eV in the high-resolution spectrum of Ag are corresponded to 3d_{5/2}} and Ag 3d_{3/2}} and show Ag⁺ and Ag⁰ states, respectively (Fig. 4d). The two characteristic peaks at 198.9 and 197.3 eV in Fig. 4e are corresponded to the Cl 2p_{1/2}} and Cl 2p_{3/2}} orbitals of Cl.

3.5. Photoluminescence

Photoluminescence technique is used to study the separation and recombination process of excited charges in semiconductors. The PL spectra of ZnO and ZnO-Ag/AgCl-30% are shown in Fig. 5. The two samples show strong fluorescence emission peaks at 539 nm, which is caused by the near band-edge emission of the intrinsic wide band gap of ZnO, as a result of the recombination of excitonic centers [38]. PL intensities are significantly quenched when Ag/AgCl is introduced on the surface of ZnO. The PL intensity of ZnO is the highest indicating poor charge separation in pure ZnO. However, the introduction of Ag/AgCl results in marked decrease in the PL intensities and the lowest intensity is provided by ZnO-Ag/AgCl-30% indicating that charge recombination has been significantly decreased in the sample which plays very important role in photocatalysis.

3.6. Photocatalytic activity

The photocatalytic degradation activities of the fabricated samples under visible light are given in Fig. 6. The degradation efficiency of ZnO is very low because of its low and weak visible light absorption. When Ag is introduced

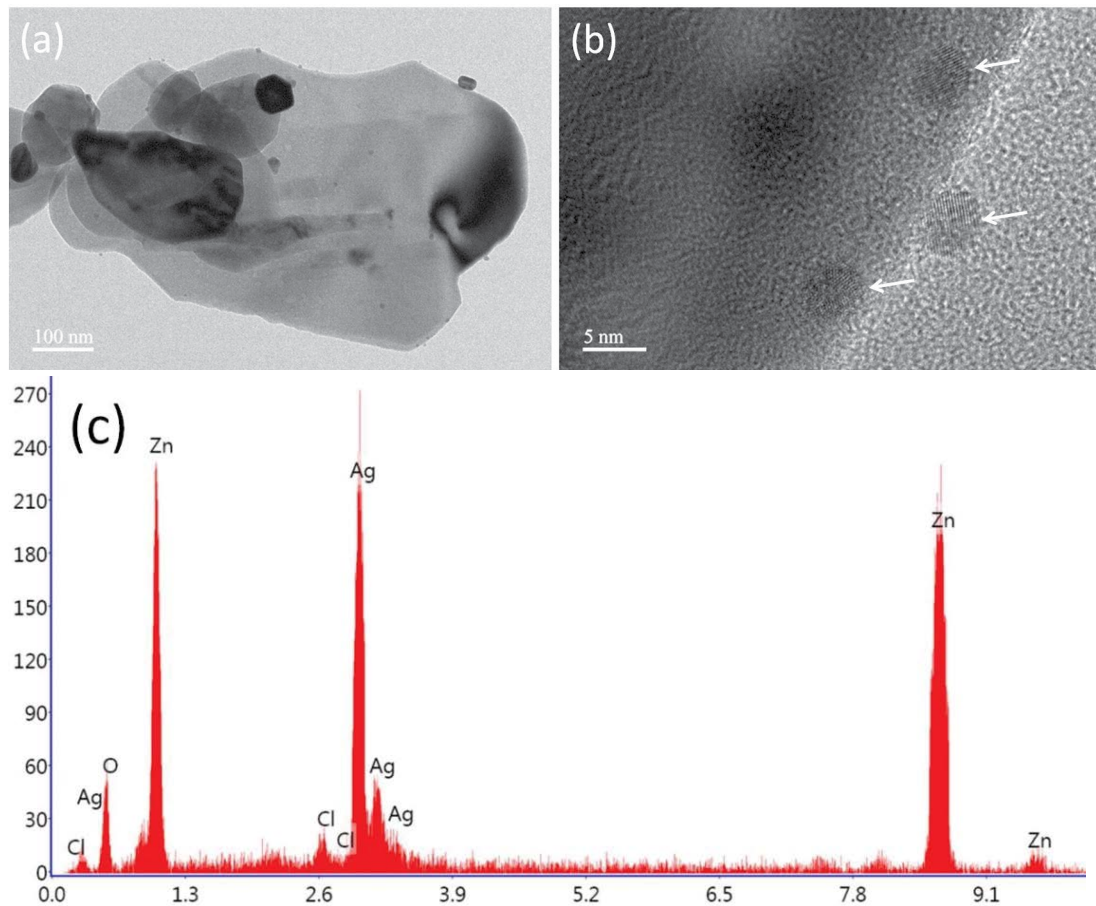


Fig. 2. TEM (a) and HRTEM (b) of ZnO-Ag/AgCl-30%, (c) corresponding EDS spectrum.

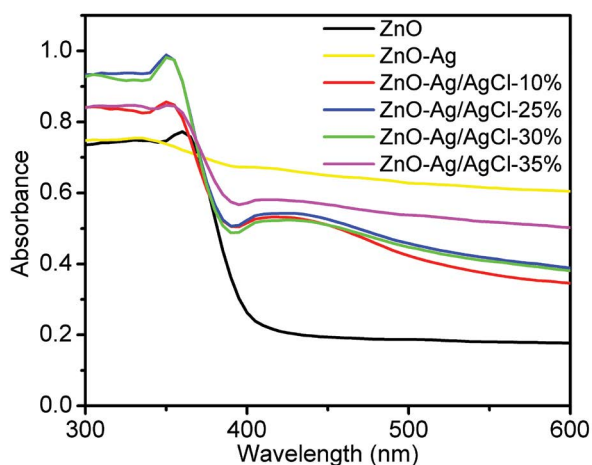


Fig. 3. UV-DRS spectrum of pure ZnO and ZnO-Ag/AgCl samples.

on the surface of ZnO, its degradation activity is significantly improved because of the visible light absorption due to the surface plasmon resonance characteristics of Ag metal and 36.2% of the pollutant is degraded in 2 h (Fig. 6a). In order to study the quantitative analysis of the prepared

photocatalysts, the apparent rate constant (k) for the photodegradation of TC-HCl was calculated based the initial 40 min (Fig. 6b). The photocatalytic activities are further improved when AgCl is cropped along with Ag on the surface of ZnO. The photocatalytic activities are increased as the amount of Ag/AgCl is increased and 80.7% of the pollutant is degraded by the ZnO-Ag/AgCl-30% sample in 2 h. However, when the amount of Ag/AgCl is increased to 35%, the degradation efficiency is slightly decreased due to aggregation of particles and their shadow effect [39]. These enhanced activities are attributed to the synergetic effect of both Ag and AgCl to absorb visible light photons and prolong the life of excited charges. As a result, the organic pollutants can occupy the active sites more frequently to utilize more photo-generated electron-hole pairs for the degradation process.

3.7. Effect of catalyst amount

The effect of the dosage of the photocatalysts on the degradation of TC-HCl is shown in Fig. 7. It is clear that the pollutant is removed rapidly in the initial stage of the photocatalysis, and this trend becomes gentle later on. When the dosage is 20 mg (0.4 g/L), the photocatalytic removal of pollutant is slow as the number of solar photons absorbed are relatively fewer to produce enough active free radicals such as h^+ , e^- , $\cdot O_2^-$, $\cdot OH$ for the degradation process. When

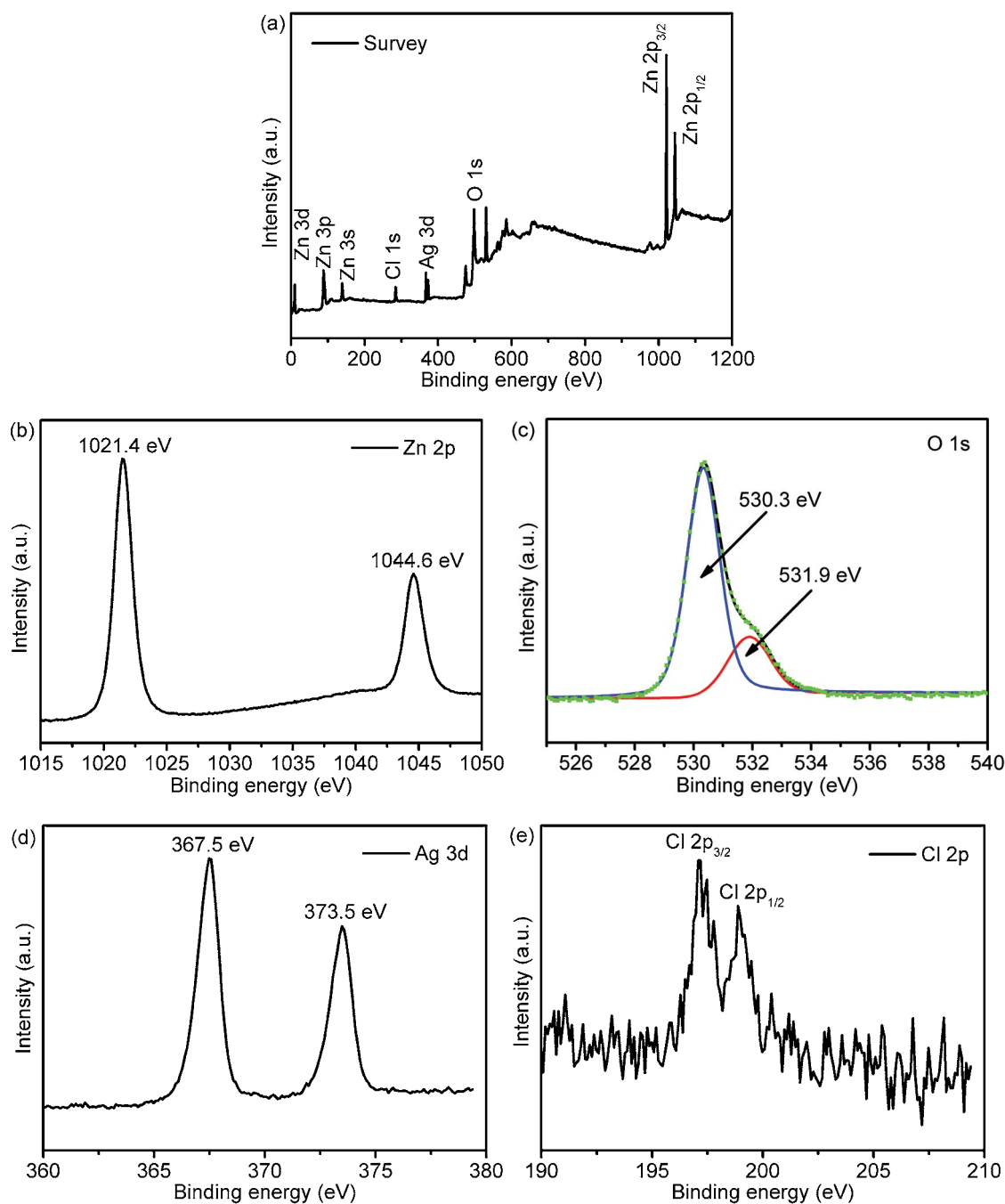


Fig. 4. XPS spectrum of the ZnO-Ag/AgCl-30% sample.

the dosage of the catalyst is increased to 32 mg (0.64 g/L), the amount of the free radical produced under light irradiation is also increased to bring the highest degradation activity. When the dosage is 40 mg (0.8 g/L), the catalytic effect is significantly reduced. This is attributed to the aggregation of the particles of the catalyst which decreases the surface area for effective adsorption of the pollutants. Moreover, too much catalyst results in light shielding phenomenon which reduces light transmittance through the solution. Thus degradation of the pollutant is decreased at high dosage of the catalyst.

3.8. Active species analysis

In order to explore the active degrading species involved in the decomposition of TC-HCl pollutant, free radical capturing experiments were carried out. Ascorbic acid, methanol, and iso-propyl alcohol (IPA) were used as quenching agents for $\cdot\text{O}_2^-$, h^+ and $\cdot\text{OH}$, respectively. Fig. 8 shows the results and photocatalytic degradation rate of TC-HCl by ZnO-Ag/AgCl-30% in the presence of different scavengers. When ascorbic acid is added to the solution, the degradation effect of ZnO-Ag/AgCl-30% on TC-HCl is greatly reduced.

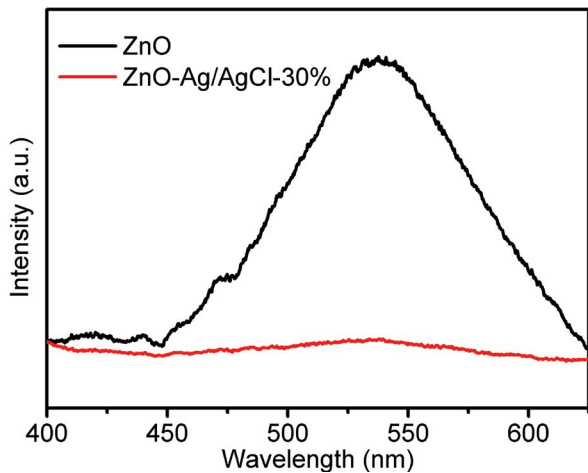


Fig. 5. PL spectrum of ZnO and ZnO-Ag/AgCl-30% samples.

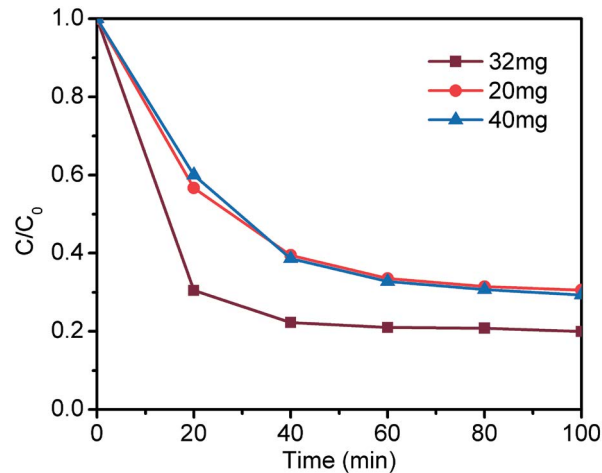


Fig. 7. Photocatalytic degradation of TC-HCl by different amounts of ZnO-Ag/AgCl-30%.

This indicates that $\cdot O_2^-$ plays an important role in the degradation of TC-HCl. When methanol is used as h^+ scavenger, the photocatalytic activity is decreased slightly compare to the degradation activity in the presence of ZnO-Ag/AgCl-30%. When IPA is added into the reaction solution, the effect on the photocatalytic degradation is higher and the photocatalytic efficiencies decreases by 10% even in 60 min irradiation, which indicates that h^+ and $\cdot OH$ are not the main species affecting the photocatalytic activity. Thus, the main active species affecting photocatalytic activity is $\cdot O_2^-$.

3.9. Photocatalytic mechanism

Based on the obtained results, we proposed a schematic of charge transfer for the process of photocatalytic degradation of TC-HCl using ZnO-Ag/AgCl under visible light irradiation (Fig. 9). When the frequency of the incident light coincides with that of the electron oscillation, the positive and negative charges are produced in Ag metal.

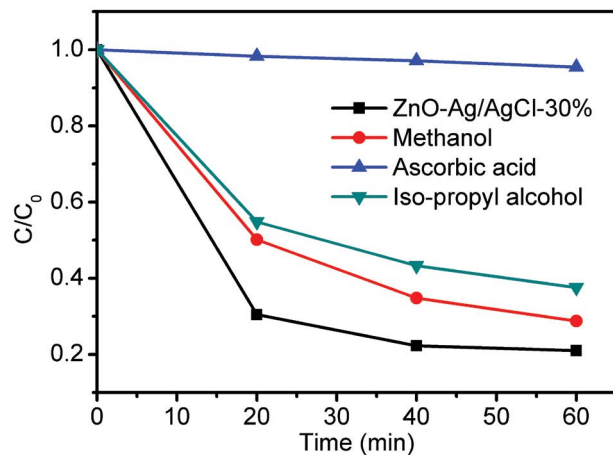


Fig. 8. Photocatalytic degradation of TC-HCl by ZnO-Ag/AgCl-30% with capturing agent.

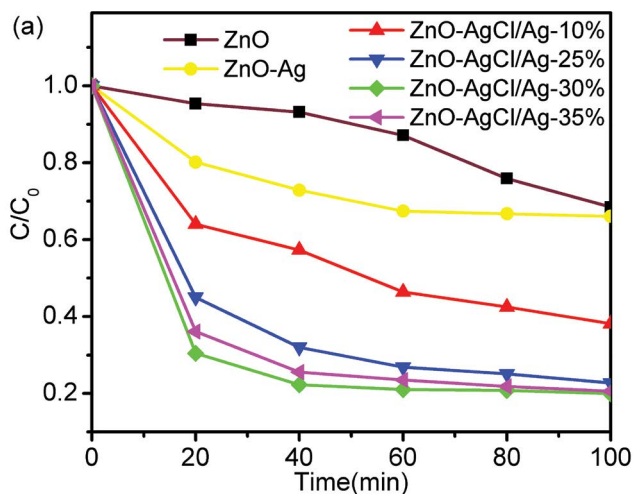


Fig. 6. Photocatalytic degradation of TC-HCl by ZnO, ZnO-Ag, ZnO-Ag/AgCl.

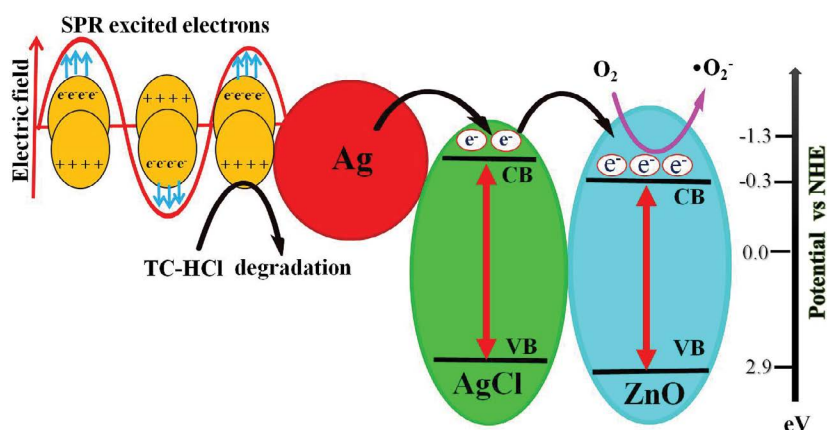


Fig. 9. The proposed photocatalytic mechanism for the ZnO-Ag/AgCl composite.

This instantaneous generation of positive and negative charges in Ag metal due to light absorption is attributed to the surface plasmon resonance phenomenon which is a distinguishing property of noble metals like Ag and plays very important role in charge separation and ultimately in photocatalysis. The surface plasmon resonance excited electrons in the Ag Fermi level possess high thermodynamic energy and are quickly transformed to the conduction band of AgCl first and then to ZnO under the action of the interface electric field. The synergistic interaction between the surface plasmon resonance (SPR) generated by silver metal with the polarized field around AgCl enforce the SPR excited electrons to ease the photogenerated charge separation and interfacial photogenerated charge transfer. This result in the photosensitization of ZnO and the transmitted electrons in the conduction band of ZnO still possess enough thermodynamic energy to generate super oxide anions from the adsorbed oxygen molecules and participate the photocatalytic degradation of TC-HCl. At the same time, the positive holes left on Ag metal (Fermi level) participate in the generation of $\cdot\text{OH}$ free radicals from water and further oxidize and decompose the adsorbed TC-HCl molecules. Thus Ag metal not only photosensitized ZnO to improve charge separation but also plays important role in the production of highly efficient degrading species for improved photocatalytic degradation of TC-HCl pollutant.

4. Conclusion

ZnO-Ag/AgCl composite was synthesized by in-situ coprecipitation and hydrothermal method, and used for the oxidation of TC-HCl under visible light irradiation. The photocatalytic activity of the nanocomposite was higher than pure ZnO. These improved photocatalytic activities are related to the surface plasmon resonance effect of Ag metal and charge separation in the nanocomposite material. Finally, charge transfer mechanism was proposed based on the obtained results and active species involved in the degradation process. The optimized sample degraded 80.7% TC-HCl in 120 min under visible light irradiation. From trapping experiments, it was concluded that super oxide anions and holes were the

main degrading species involved in the degradation of TC-HCl. In conclusion, the synthesized ZnO-Ag/AgCl has a good potential for environmental remediation.

Notes

The authors declare no competing financial interest.

Acknowledgement

This work was supported by Education Office of Liaoning Province (LQN201712, LJKZ0997), Liaoning Revitalization Talents Program (XLYC1807238), Liaoning BaiQianWan Talents Program (2020921111), Natural Science Foundation of Liaoning Province (2020-MS-312), Key Laboratory of Advanced Energy Materials Chemistry (Ministry of Education) (111 project, B12015), the National Natural Science Foundation of China (22075186, 21975164).

References

- [1] F. Al Marzouqi, Y. Kim, R. Selvaraj, Shifting of the band edge and investigation of charge carrier pathways in the CdS/g-C₃N₄ heterostructure for enhanced photocatalytic degradation of levofloxacin, *New J. Chem.*, 43 (2019) 9784–9792.
- [2] H. Chen, L. Jing, Y. Teng, J. Wang, Multimedia fate modeling and risk assessment of antibiotics in a water-scarce megacity, *J. Hazard. Mater.*, 348 (2018) 75–83.
- [3] R. He, J. Zhou, H. Fu, S. Zhang, C. Jiang, Room-temperature in situ fabrication of Bi₂O₃/g-C₃N₄ direct Z-scheme photocatalyst with enhanced photocatalytic activity, *Appl. Surf. Sci.*, 430 (2018) 273–282.
- [4] K. Qi, B. Cheng, J. Yu, W. Ho, A review on TiO₂-based Z-scheme photocatalysts, *Chin. J. Catal.*, 38 (2017) 1936–1955.
- [5] W. Li, C. Zhuang, Y. Li, C. Gao, W. Jiang, Z. Sun, K. Qi, Anchoring ultra-small TiO₂ quantum dots onto ultra-thin and large-sized Mxene nanosheets for highly efficient photocatalytic water splitting, *Ceram. Int.*, 47 (2021) 21769–21776.
- [6] K. Qi, S.-y. Liu, R. Selvaraj, W. Wang, Z. Yan, Comparison of Pt and Ag as co-catalyst on g-C₃N₄ for improving photocatalytic activity: experimental and DFT studies, *Desal. Water Treat.*, 153 (2019) 244–252.
- [7] F.S. Ali, K. Qi, B. Al Wahaibi, M.A. Meetani, H. Al Lawati, Y. Kim, S.M.Z. Al Kindy, R. Selvaraj, Photocatalytic degradation of bisphenol A in the presence of TiO₂ nanoparticle: effect of solvent on size control, *Desal. Water Treat.*, 79 (2017) 301–307.

- [8] K. Qi, S.-y. Liu, R. Wang, Z. Chen, R. Selvaraj, Pt/g-C₃N₄ composites for photocatalytic H₂ production and •OH formation, *Desal. Water Treat.*, 154 (2019) 312–319.
- [9] X. Li, J. Xiong, Y. Xu, Z. Feng, J. Huang, Defect-assisted surface modification enhances the visible light photocatalytic performance of g-C₃N₄@C-TiO₂ direct Z-scheme heterojunctions, *Chin. J. Catal.*, 40 (2019) 424–433.
- [10] N. Kumaresan, M.M.A. Sinthiya, M. Sarathbavan, K. Ramamurthi, K. Sethuraman, R.R. Babu, Synergetic effect of g-C₃N₄/ZnO binary nanocomposites heterojunction on improving charge carrier separation through 2D/1D nanostructures for effective photocatalytic activity under the sunlight irradiation, *Sep. Purif. Technol.*, 244 (2020) 116356.
- [11] K. Qi, A. Zada, Y. Yang, Q. Chen, A. Khataee, Design of 2D–2D NiO/g-C₃N₄ heterojunction photocatalysts for degradation of an emerging pollutant, *Res. Chem. Intermed.*, 46 (2020) 5281–5295.
- [12] T. Usharani, R. Baskar, B. Palanisamy, M. Myilsamy, Efficient photocatalytic degradation of 2,4-dinitrophenol over mesoporous Zr and Ce co-doped TiO₂ under visible light, *Desal. Water Treat.*, 217 (2021) 320–328.
- [13] C. Djilani, R. Zaghdoudi, F. Djazi, A. Lallam, B. Boucekima, P. Magri, Comparative study of photocatalytic activity of nanocomposites prepared from biological wastes and ZnO nanoparticles, *Desal. Water Treat.*, 220 (2021) 329–341.
- [14] K. Qi, S.-y. Liu, A. Zada, Graphitic carbon nitride, a polymer photocatalyst, *J. Taiwan Inst. Chem. Eng.*, 109 (2020) 111–123.
- [15] H. Zhang, Y. Li, W. Li, C. Zhuang, C. Gao, W. Jiang, W. Sun, K. Qi, Z. Sun, X. Han, Designing large-sized cocatalysts for fast charge separation towards highly efficient visible-light-driven hydrogen evolution, *Int. J. Hydrogen Energy*, 46 (2021) 28545–28553.
- [16] K. Qi, N. Cui, M. Zhang, Y. Ma, G. Wang, Z. Zhao, A. Khataee, Ionic liquid-assisted synthesis of porous boron-doped graphitic carbon nitride for photocatalytic hydrogen production, *Chemosphere*, 272 (2021) 129953.
- [17] M. Sait Çevik, Ö. Şahin, O. Baytar, S. Horoz, A. Ekinci, Investigation of the effect of magnesium and activated carbon on the photocatalytic degradation reaction of ZnO photocatalyst, *Desal. Water Treat.*, 209 (2021) 212–218.
- [18] S.-y. Liu, J. Ru, F. Liu, NiP/CuO composites: electroless plating synthesis, antibiotic photodegradation and antibacterial properties, *Chemosphere*, 267 (2021) 129220.
- [19] T. Ilyas, F. Raziq, N. Ilyas, L. Yang, S. Ali, A. Zada, S.H. Bakhtiar, Y. Wang, H. Shen, L. Qiao, FeNi@CNS nanocomposite as an efficient electrochemical catalyst for N₂-to-NH₃ conversion under ambient conditions, *J. Mater. Sci. Technol.*, 103 (2022) 59–66.
- [20] K. Qi, X. Xing, A. Zada, M. Li, Q. Wang, S.-y. Liu, H. Lin, G. Wang, Transition metal doped ZnO nanoparticles with enhanced photocatalytic and antibacterial performances: Experimental and DFT studies, *Ceram. Int.*, 46 (2020) 1494–1502.
- [21] C. Gonçalves, K.B. Fontana, M.A.R. Tenorio, V.L.A.F. Bascuñán, G.G. Lenzi, E.S. Chaves, Zinc oxide immobilized on alginate beads as catalyst for photocatalytic degradation of textile dyes – an evaluation of matrix effects, *Desal. Water Treat.*, 210 (2021) 250–257.
- [22] L. Miao, B. Shi, N. Stanislaw, C. Mu, K. Qi, Facile synthesis of hierarchical ZnO microstructures with enhanced photocatalytic activity, *Mater. Sci.-Poland*, 35 (2017) 45–49.
- [23] K. Saeed, I. Khan, M. Ahad, T. Shah, M. Sadiq, A. Zada, N. Zada, Preparation of ZnO/Nylon 6/6 nanocomposites, their characterization and application in dye decolorization, *Appl. Water Sci.*, 11 (2021), doi: 10.1007/s13201-021-01442-0.
- [24] N.V. Suc, Photocatalytic degradation of 1:2 metal complex dye acid blue 193 under solar light condition using ZnO nanoneedles and ZnO/bentonite nanocomposite synthesized via microwave irradiation, *Desal. Water Treat.*, 228 (2021) 414–421.
- [25] A. Zada, M. Khan, Z. Hussain, M.I.A. Shah, M. Ateeq, M. Ullah, N. Ali, S. Shaheen, H. Yasmeen, S.N. Ali Shah, A. Dang, Extended visible light driven photocatalytic hydrogen generation by electron induction from g-C₃N₄ nanosheets to ZnO through the proper heterojunction, *Z. Phys. Chem.*, (2021), doi: 10.1515/zpch-2020-1778.
- [26] K. Qi, B. Cheng, J. Yu, W. Ho, Review on the improvement of the photocatalytic and antibacterial activities of ZnO, *J. Alloys Compd.*, 727 (2017) 792–820.
- [27] H. Yasmeen, A. Zada, S. Ali, I. Khan, W. Ali, W. Khan, M. Khan, N. Anwar, A. Ali, A.M. Huerta-Flores, F. Subhan, Visible light-excited surface plasmon resonance charge transfer significantly improves the photocatalytic activities of ZnO semiconductor for pollutants degradation, *J. Chin. Chem. Soc.*, 67 (2020) 1611–1617.
- [28] Z. Xu, N. Liu, Y. Han, P. Zhang, Z. Hong, J. Li, Preparation of Ag/ZnO microspheres and study of their photocatalytic effect on dichloromethane, *Desal. Water Treat.*, 216 (2021) 162–169.
- [29] Y. Humaira, Z. Amir, L. Shouxin, Surface plasmon resonance electron channeled through amorphous aluminum oxide bridged ZnO coupled g-C₃N₄ significantly promotes charge separation for pollutants degradation under visible light, *J. Photochem. Photobiol., A*, 400 (2020) 112681.
- [30] L. Liu, G. Zhao, C. Li, S. Zhou, Y. Wang, F. Jiao, Synthesis of N-doped ZnO/ZnCo₂O₄ composites for stable photocatalytic degradation of organic dyes, *Desal. Water Treat.*, 217 (2021) 411–421.
- [31] S.S. Madani, A. Habibi-Yangjeh, S. Asadzadeh-Khaneghah, H. Chand, V. Krishnan, A. Zada, Integration of Bi₂O₃ nanoparticles with ZnO: impressive visible-light-induced systems for elimination of aqueous contaminants, *J. Taiwan Inst. Chem. Eng.*, 119 (2021) 177–186.
- [32] Y. Xu, L. Zhang, J. Chen, Y. Fu, Q. Li, J. Yin, Z. Cheng, W. Kan, P. Zhao, H. Zhong, Y. Zhao, X. Wang, Synthesis of nano-Ag-assisted attapulgite/g-C₃N₄ composites with superior visible light photocatalytic performance, *Mater. Chem. Phys.*, 221 (2019) 447–456.
- [33] S. Zhang, I. Khan, X. Qin, K. Qi, Y. Liu, S. Bai, Construction of 1D Ag-AgBr/AlOOH plasmonic photocatalyst for degradation of tetracycline hydrochloride, *Front. Chem.*, 8 (2020) 117.
- [34] Z. Zhang, A. Zada, N. Cui, N. Liu, M. Liu, Y. Yang, D. Jiang, J. Jiang, S. Liu, Synthesis of Ag loaded ZnO/BiOCl with high photocatalytic performance for the removal of antibiotic pollutants, *Crystals*, 11 (2021) 981.
- [35] M. Malakootian, S.N. Asadzadeh, M. Mehdipoor, D. Kalantar-Neyestanaki, A new approach in photocatalytic degradation of tetracycline using biogenic zinc oxide nanoparticles and peroxydisulfate under UVC irradiation, *Desal. Water Treat.*, 222 (2021) 302–312.
- [36] S. Liu, J. Wang, J. Yu, ZIF-8 derived bimodal carbon modified ZnO photocatalysts with enhanced photocatalytic CO₂ reduction performance, *RSC Adv.*, 6 (2016) 59998–60006.
- [37] J. Wang, Y. Xia, Y. Dong, R. Chen, L. Xiang, S. Komarneni, Defect-rich ZnO nanosheets of high surface area as an efficient visible-light photocatalyst, *Appl. Catal., B*, 192 (2016) 8–16.
- [38] L. Wang, L. Chang, B. Zhao, Z. Yuan, G. Shao, W. Zheng, Systematic investigation on morphologies, forming mechanism, photocatalytic and photoluminescent properties of ZnO nanostructures constructed in ionic liquids, *Inorg. Chem.*, 47 (2008) 1443–1452.
- [39] K. Qi, Y. Xie, R. Wang, S.-y. Liu, Z. Zhao, Electroless plating Ni-P cocatalyst decorated g-C₃N₄ with enhanced photocatalytic water splitting for H₂ generation, *Appl. Surf. Sci.*, 466 (2019) 847–853.